South African Journal for Science and Technology
ISSN: (Online) 2222-4173, (Print) 0254-3486

Lithium extraction from Zimbabwean petalite using ammonium bifluoride

Authors:
KT Mwepu
SJ Lubbe
PL Crouse

Affiliations:
Department of Chemical Engineering, University of Pretoria, Lynnwood Road, Pretoria, 0002, South Africa

Corresponding author:
KT Mwepu
E-mail:
titemwepu@gmail.com

Dates:
Received: 20/07/20
Accepted 20/01/21
Published: 31/05/21

How to cite this article:
KT Mwepu, SJ Lubbe, PL Crouse, Lithium extraction from Zimbabwean petalite using ammonium bifluoride, *Suid-Afrikaanse Tydskrif vir Natuurwetenskap en Tegnologie* 40(1) (2021). https://doi.org/10.36303/SATNT.2021.40.1.800

'n Afrikaanse vertaling van die manuskrip is aanlyn beskikbaar by http://www.satnt.ac.za/index.php/satnt/article/view/800

Copyright:
© 2021. Authors. Licensee: *Die Suid-Afrikaanse Akademie vir Wetenskap en Kuns*. This work is licensed under the Creative Commons Attibution License.

Extraction of Li_2CO_3 from Zimbabwean petalite, from the Bikita deposit, was studied using ammonium bifluoride (ABF) digestion at temperatures ranging from room temperature to 600 °C, and gram quantities of ore. ABF digestion bypasses the conventional high-temperature conversion of the mineral to β-spodumene before acid roasting. The process reaction takes place at surprisingly low temperatures – even at room temperature with slurry formation due to the release of water. Below the melting point of ABF, the main products are LiF, AlF_3, K_2NaAlF_6, and $(NH_4)_2SiF_6$. $(NH_4)_2SiF_6$ decomposes readily to form ammonia and gaseous SiF_4. At higher temperature, the products are cryolithionite ($Li_3Na_3Al_2F_{12}$) and eucryptite ($LiAlSiO_4$). The fluoride solids are not readily soluble in water and may be roasted in sulfuric acid at relatively mild conditions for a few tens of minutes, then water leached, with 99 % pure lithium carbonate easily recovered from the aqueous phase.

Keywords: petalite, digestion, leaching, purification, precipitation, lithium carbonate, Bikita minerals

Litium-ontginning uit Zimbabwiese petaliet met behulp van ammoniumbifluoried: Hierdie studie behels die ontginning van gramhoeveelhede Li_2CO_3 uit Zimbabwiese petaliet, gemyn in die Bikita-gebied. Ekstraksie is gedoen met behulp van ammoniumbifluoried (ABF), vanaf kamertemperatuur tot 600 °C. ABF-vertering vervang die konvensionele hoëtemperatuurproses vir die omsetting van die mineraal na β-spodumeen voor suurbehandeling. Die ABF-proses vind by verrassende lae temperature plaas – selfs by kamertemperatuur word floddervorming waargeem as gevolg van die water wat tydens die reaksie vorm. Onder die smeltpunt van ABF is die hoofreaksieprodukte LiF, AlF_3, K_2NaAlF_6, en $(NH_4)_2SiF_6$. $(NH_4)_2SiF_6$ ontbind geredelik om ammoniak en gasagtige SiF_4 te vorm. By laer temperature is die produkte kriolitioniet ($Li_3Na_3Al_2F_{12}$) and eukriptiet ($LiAlSiO_4$). Die fluoriedhoudende vastestowwe is swak oplosbaar in water. Die mengsel moet met swawelsuur gerooster word, en daarna word die sulfate met water uitgeloog; 99 % suiwer litiumkarbonaat word relatief maklik uit die waterige fase herwin.

Sleutelterme: petaliet, vertering, loog, suiwering, presipitasie, litiumkarbonaat, Bikita Minerals

Introduction

Since the end of World War II, lithium production has steadily increased, more recently due to the use of the element in lithium-ion batteries for portable electronics and for electric vehicle applications (Hui et al., 2019). Hien-Dinh et al. (2015) predict an annual increase in lithium demand of 9.7 %. Kuang et al. (2018) predict worldwide lithium consumption to increase by 20 % per year through 2020. The most common sources of lithium are salts in surface and subsurface brines as well as pegmatite minerals like spodumene, zinnwaldite, lepidolite, amblygonite and petalite. These are considered as the most economically viable Li-containing minerals in the world (Garrett, 2004, Linnen et al., 2012, Aylmore et al., 2018). Petalite, as the most sought-after lithium-bearing mineral due to its high lithium content, can be used to extract and produce compounds such as lithium carbonate (Li_2CO_3), lithium chloride (LiCl), and lithium fluoride (LiF) (Sitando and Crouse, 2012). Petalite mineral deposits are found in Australia, Namibia, Canada, Russia, and Zimbabwe.

Lithium carbonate is considered to be the precursor to other lithium compounds and the feed chemical for lithium metal production (Jandová et al., 2010). LiF has applications in specialised UV optics, ceramics, and the aluminium smelting process. LiCl is a source for lithium metal via electrolysis of LiCl/KCl at 450 °C or as a flux for aluminium in automobile parts and a desiccant for drying air streams.

Conventionally, lithium extraction from petalite starts with heat treatment of the mineral at 1100 °C for at least 2 h to convert the monoclinic crystal structure into acid-soluble β-spodumene. It is energy-intensive and costly (Guo et al., 2019, Hui et al., 2019, Rosales et al., 2013, Rosales et al., 2016). The lithium is extracted as lithium sulfate (Li_2SO_4), along with several contaminants, via roasting of the β-spodumene with sulfuric acid at 300 °C for 60 min. To arrive at a final product, typically lithium carbonate, the aqueous Li_2SO_4 is filtered, to remove the insoluble silicates, and purified by selective precipitation of the contaminants as hydroxides. To achieve this, the pH is raised, usually using calcium carbonate or hydroxide. Finally, the lithium carbonate is precipitated by the addition of sodium carbonate (Garrett, 2004, Hien-Dinh et al., 2015, Kondás et al., 2006, Guo et al., 2019, Sitando and Crouse, 2012, Wietelmann and Bauer, 2003).

As an alternative to the heat-treatment step, Guo et al. (2019) published a study on lithium extraction from α-spodumene using hydrogen fluoride (HF) as a digesting agent. The results showed that HF reacts with α-spodumene, breaking the oxide bonds forming cryolithionite ($Na_3Li_2Al_2F_{12}$), cryolite (Na_3AlF_6), calcium fluoride (CaF_2), potassium cryolite (K_2AlF_5), aluminium fluoride (AlF_3) which can be dissolved in H_2SO_4, and fluorosilicates (Na_2SiF_6 or $KNaSiF_6$). HF was used in these studies as the principal source of fluorine, at a relatively low temperature.

However, according to Andreev et al. (2007a), HF requires special working conditions since it results in the emission of toxic gases such as SiF_4 and effluents with high concentrations of fluoride ions (Rosales et al., 2013). ABF-based processes are less problematic since even just above its melting point it still has a very low vapour pressure, whereas HF is a gas at room temperature. A specialist knowledge of fluorochemical processing is required for any fluorine-related process.

A number of articles on the dissolution of silicate compound using ammonium bifluoride (ABF) have also been published (Andreev et al., 2007a, Andreev et al., 2007b, Du Plessis et al., 2016, Nel et al., 2011, Nhlabathi et al., 2012, Retief et al., 2014). These authors used ABF as a source of anhydrous hydrogen fluoride (AHF) for the dissolution of silica-containing minerals at varying decomposition temperatures and pressures. Retief et al. (2014) claimed the separation of silicon from a zirconia-based material using ABF to produce ammonium heptafluorozirconate ($(NH_4)_3ZrF_7$) and ammonium hexafluorosilicate $(NH_4)_2SiF_6$. The latter compound can be thermally decomposed. Nel et al. (2011) and Du Plessis et al. (2016) respectively studied reaction kinetics between plasma-dissociated zircon and ABF, also forming ($(NH_4)_3ZrF_7$) and $(NH_4)_2SiF_6$. Nhlabathi et al. (2012) extended the work reported by Nel et al. (2011) in order to refine the kinetics. In general, ABF is used in its molten state, as facile source of AHF. In the case of topaz, the reaction results in the formation of ammonium hexafluorosilicate and ammonium hexafluoroaluminate (Andreev et al., 2007a):

$$Al_2(SiO_4)F_{2\,(s)} + 8NH_4F.HF_{(s)} \rightarrow (NH_4)_2SiF_{6(g)} + 4H_2O_{(l)} + 2(NH_4)_3AlF_{6(s)} \quad (1)$$

Ammonium hexafluorosilicate and hexafluoroaluminate can be thermally decomposed according to:

$$(NH_4)_2SiF_{6(g)} \rightarrow SiF_{4(g)} + 2NH_{3(g)} + 2HF_{(g)} \quad (2)$$

$$(NH_4)_3AlF_{6(s)} \rightarrow AlF_{3(s)} + 3NH_{3(g)} + 3HF_{(g)} \quad (3)$$

The aim of the research reported here was to assess whether ABF may be used to extract lithium from petalite without the initial thermal conversion to β-spodumene. Results of benchtop experiments are reported in this paper. ABF was reacted with petalite and the product mixture purified to yield lithium carbonate. Characterisation of reagents and materials was done by inductively-coupled plasma optical emission spectroscopy (ICP-OES), X-ray diffractometry (XRD), and X-ray fluorescence spectrometry (XRF).

Experimental

Materials and reagents

The petalite was sourced from Bikita Minerals (Pvt) Ltd in Zimbabwe. Analytical grade NH_4HF_2 and H_2SO_4 from Merck Chemicals were used. Deionised water was used for all aqueous applications.

Instrumentation

A Spectro Arcos ICP-OES was employed for lithium analysis. A Thermo ARL9400 XP XRF spectrometer was used to determine the elemental composition of the petalite concentrate. A PANalytical XRD was used to determine the mineral phases of the petalite concentrate. Analysis was perfumed using Fe filtered Co Kα as a radiation source. The phases were identified using X'Pert Highscore Plus software. The reference intensity method in the X'Pert Highscore Plus software was used to estimate the semi-quantitative phase amounts (weight %). A Hitachi 7300 was used for the thermogravimetric analysis (TGA) of ABF. A Perkin-Elmer Spectrum 100 Fourier-transform infrared spectrophotometer (FTIR) was used to obtain vibrational spectra. A Mettler PM2000MC balance was used for weighing. pH measurements were done with a pH meter model Adwa AD 111. Particle size analysis was performed using a Malvern Mastersizer 3000.

Experimental method

At temperatures between 25 °C and 100 °C, digestion was done by mixing 5 g of petalite ($LiAlSi_{14}O_{10}$) with 37.5 g of ABF (NH_4HF_2) in polytetrafluoroethylene (PTFE) containers. The furnace was preheated to the desired temperature and when its temperature reached the pre-set value and remained stable, the containers along with the mixture were inserted and left for the set period. To quench the reaction, 3–5 times excess by volume water was added to the reaction product to dissolve the water-soluble products and filtered. The remaining solid was dried at 100 °C and weighed. These insoluble products were mixed with a 10% excess sulfuric acid and roasted at 200 °C for 30 min. The resulting product was cooled to room temperature, water was added and dissolved at 80 °C for 20 min. The reaction between petalite and ABF, can be represented by Reaction (4) below ($\Delta_{Rxn}G°_{298}$ = -13089.7 kJ mol^{-1}):

$$Li_2OAl_2O_38SiO_{2(s)} + 40NH_4HF_{2(s)} \rightarrow 2LiF_{(s)} + 2AlF_{3(s)} + 8\,(NH_4)_2SiF_{6(s)} + 24\,NH_4F_{(aq)} + 20H_2O_{(l)} \quad (4)$$

In this reaction the product water molecules do not evaporate and the ammonium fluoride is assumed to still be present either fully or partially dissolved in the product water. Note again that ammonium hexafluorosilicate is easily decomposed thermally, to yield NH_3 (g), HF (g) and SiF_4 (g). The acid roasting reaction of lithium fluoride/aluminium fluoride with H_2SO_4 is shown in Reaction (5) ($\Delta_{Rxn}G°_{298}$ = -6817.25 kJ mol^{-1}) (Kuang et al., 2012).

$$2LiF_{(s)} + 2AlF_{3(s)} + 4H_2SO_{4(l)} \rightarrow Li_2SO_{4(s)} + Al_2(SO_4)_{3(s)} + 8HF_{(g)} \quad (5)$$

Lithium sulfate and aluminium sulfate are water soluble. After filtration, the filtrate was used to determine the lithium concentration by ICP-OES. All experiments were done in triplicate.

At temperatures between 200 °C and 600 °C stoichiometric ratios were used. Digestion was done using 5 g of petalite ($LiAlSi_{14}O_{10}$) and 12.26 g of ABF in polytetrafluoroethylene containers. The furnace was heated to the desired temperature with the containers inserted and kept there for 2 h. To quench the reaction, water was added to the reaction product to dissolve the water-soluble products and filtered. The remaining solid was dried at 100 °C and weighed. These insoluble products were mixed with an excess sulfuric acid and roasted. The resulting product was cooled to room temperature, water was added and dissolved at 80 °C. The stoichiometric reaction between petalite and ABF can be represented following Reaction (6) below ($\Delta_{Rxn}G°_{298}$ = -10569.5 kJ mol^{-1}).

$$Li_2OAl_2O_38SiO_{2(s)} + 40NH_4HF_{2(s)} \rightarrow 2/3\ Li_3AlF_{6(s)} + 4/3\ AlF_{3(s)} + 8(NH_4)_2SiF6_{(s)} + 24NH_{3(g)} + 20H_2O_{(g)} + 24HF_{(g)} \quad (6)$$

Here the lithium and aluminium fluorides associate, and the temperature is high enough to decompose the ammonium fluoride, but not the ammonium hexafluorosilicate. Ammonium fluoride decomposes to NH_3 (g) and HF (g) at ~150 °C, while ammonium hexafluorosilicate decomposes to NH_3 (g), HF (g) and SiF_4 (g) starting from about 200 °C (see Figure 3 below). The acid roasting reaction of lithium cryolite/aluminium fluoride with H_2SO_4 is shown in Reaction (7) below ($\Delta_{Rxn}G°_{298}$ = -14333.7 kJ mol^{-1}) (Kuang et al., 2012).

$$2Li_3AlF_{6\,(s)} + 2AlF_{3\,(s)} + 9H_2SO_{4\,(l)} \rightarrow 3Li_2SO_{4\,(s)} + 2Al_2(SO_4)_{3\,(s)} + 18HF_{(g)} \quad (7)$$

The filtrate containing the lithium was used to determine the lithium and contaminant concentration by ICP-OES. All experiments were done in triplicate. The resulting solution was purified using $CaCO_3$ and $Ca(OH)_2$. Li_2CO_3 was then precipitated using Na_2CO_3.

The high-temperature results were generated as a number of one-variable-at-a-time investigations in which we varied the acid roasting temperature between 100 °C and 300 °C, the roasting time between 15 min and 45 min, the acid excess between 0 % and 20 %, the leaching stirring rate between 100 rpm and 400 rpm, the solid-liquid ratio for leaching between 0.05 g mL^{-1} and 0.13 g mL^{-1}, and the leaching time between 10 min and 40 min.

Results and discussion

Ore characterisation

The crystallographic analysis of the as-received ore is reported in Table 1. The pegmatite is composed mainly of petalite (naturally occurring in the α-phase). It also contains some associated minerals, viz. quartz, bikitaite, spodumene, lepidolite, and albite.

Figure 1 shows the particle size distribution of the material as received. 90 % is less than 74 µm, 50 % less than 27 µm and 10 % is less than 3.5 µm.

The elemental composition is shown in Table 2. The analysis was performed using XRF and ICP-OES.

TABLE 1: Semi-quantitative mineral content of the petalite (XRD analysis)

Mineral phase	(Wt. %)
Quartz (SiO_2)	6.1
Bikitaite ($LiAlSi_2O_6(H_2O)$)	7.3
Petalite ($LiAlSi_4O_{10}$)	79.9
Spodumene ($LiAlSi_2O_6$)	2.1
Lepidolite ($K(Al_{0.62}Li_{0.38})2Li0_{.92}Si_4Al0_{.42}O_{10}(OH)_{0.485}F_{1.51}$)	1.1
Albite ($NaAlSi_3O_8$)	3.5

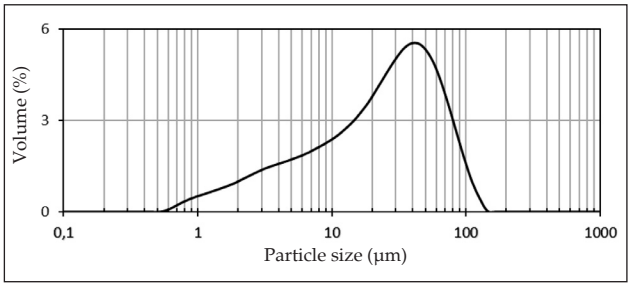

FIGURE 1: Particle size distribution of petalite determined using a Malvern Mastersizer 3000.

TABLE 2: Chemical composition of the Zimbabwean petalite using ICP-OES and XRF

Component	ICP-OES (%)	XRF (%)
SiO_2	-	78.6
Al_2O_3	-	17.8
Li_2O	4.3	-
Fe_2O_3	-	0.08
Na_2O	-	0.20
MgO	-	0.15
K_2O	-	0.14
CaO	-	0.09
Rb_2O	-	0.03
MnO	-	0.01
P_2O_5	-	0.01
ZrO_2	-	0.01
Cr_2O_3	-	0.01
SrO	-	<0.01
Co_3O_4	-	<0.01
SO_3	-	2.87
TOTAAL		**99.99**

Results for ABF digestion at temperatures higher than 100 °C

ABF digestion

The high-temperature results, between 200 °C and 600 °C, are given in Figure 2. The X-ray diffractogram of the unreacted ore is given in (a), showing a predominance of petalite ($LiAlSi_4O_{10}$), with some quartz and albite ($NaAlSi_3O_8$). In Figure 2 (b) and (c), working at 200 °C and 300 °C, the X-ray diffractograms of the residues show partial dissolution of the petalite resulting in the formation of LiF and AlF_3. From 400 °C, 500 °C and 600 °C in Figure 2 (d), (e) and (f), dissolution of petalite was almost complete. This leads to the formation of cryolithionite ($Li_3Na_3Al_2F_{12}$).

According to Rosales et al. (2013), cryolithionite formation is due to the opening of the ore during the reaction, releasing Li^+, Na^+ and Al^+ ions from petalite and albite to react with the digesting agent as shown in the equations below.

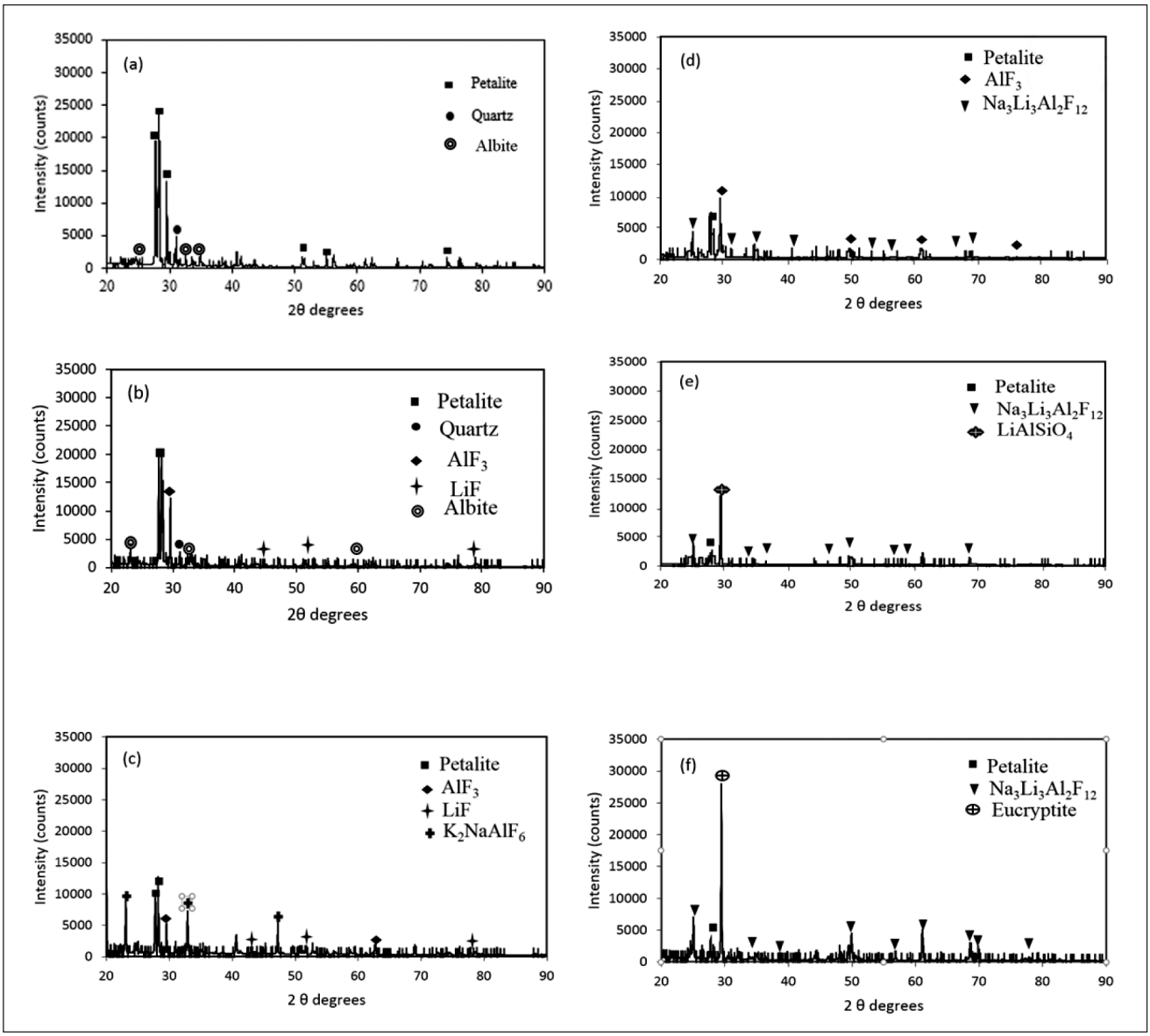

FIGURE 2: X-ray diffractogram of petalite residues obtained at the following conditions (ore/ABF ratio 1/1: (a) Zimbabwean petalite before reaction, (b) 200 °C, (c) 300 °C, (d) 400 °C, (e) 500 °C, (f) 600 °C.

$$NaAlSi_3O_{8(s)} + 11NH_4HF_{2(s)} \rightarrow NaF_{(s)} + AlF_{3(s)} + 3(NH_4)_2SiF_{6(s)} + 5NH_{3(s)} + 8H_2O_{(l)} \quad (8)$$

$$Li_3AlF_{6(s)} + AlF_{3(s)} + 3NaF_{(s)} \rightarrow Li_3Na_3Al_2F_{12(s)} \quad (9)$$

The digestion process was also studied by dynamic thermogravimetric analysis (TGA) at a constant heating rate of 10 ºC/min. The thermogram is presented in Figure 3.

Without further work, only a tentative interpretation of the observations is possible. ABF melts and starts decomposing in the range 115 °C to 220 °C (House and Engel, 1993). Up to ~150 °C, mass loss is due to ABF losses, along with water released by the reaction. Ammonium hexafluorosilicate is formed and evaporates between 230 °C and 370 °C. Between 370 °C and 1 000 °C, only solid fluorides remain, viz. cryolithionite, aluminium fluoride and eucryptite.

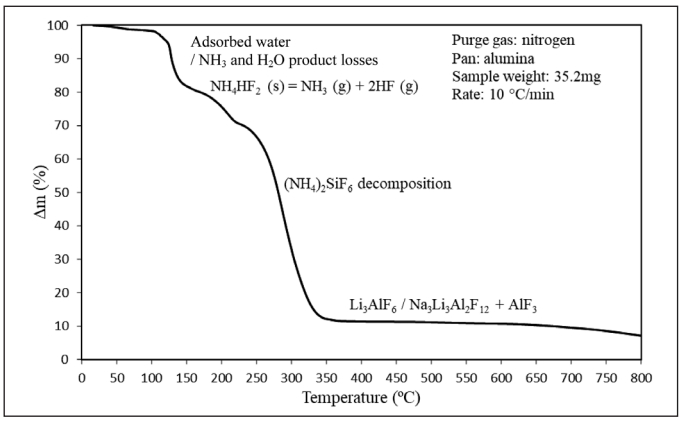

FIGURE 3: TGA of a roughly stoichiometric excess mixture of ABF and petalite

FTIR analyses of the residues after digestion were performed, as shown in Figure 4. In Figure 4 (a), the spectrum of unreacted ore, the peak at 625 cm^{-1} can be assigned to the absorption band of Si–Si, and the peaks at 1000 and 1100 cm^{-1} to the bulk Si–O–Si and Si–O modes, respectively (Hoshino and Adachi, 2007). They are still prominent at 200 °C but decrease dramatically as the treatment temperature increases, Figure 4 (c) 300 °C, (d) 400 °C, (e) 500 °C, and (f) 600 °C.

The bands observed at 1 443 cm^{-1} and 3 290 cm^{-1}, observed up to 400 °C are attributed to N-H bending and stretching respectively (Kabacelik and Ulug, 2008), evidence for the presence of undecomposed ammonium fluorometallates. At 500 °C and above, IR activity is well below 900 cm^{-1}. The peaks around 580 cm^{-1} are attributed to the formation of AlF_6^{3-} in the form of AlF_3 (Duke et al., 1990).

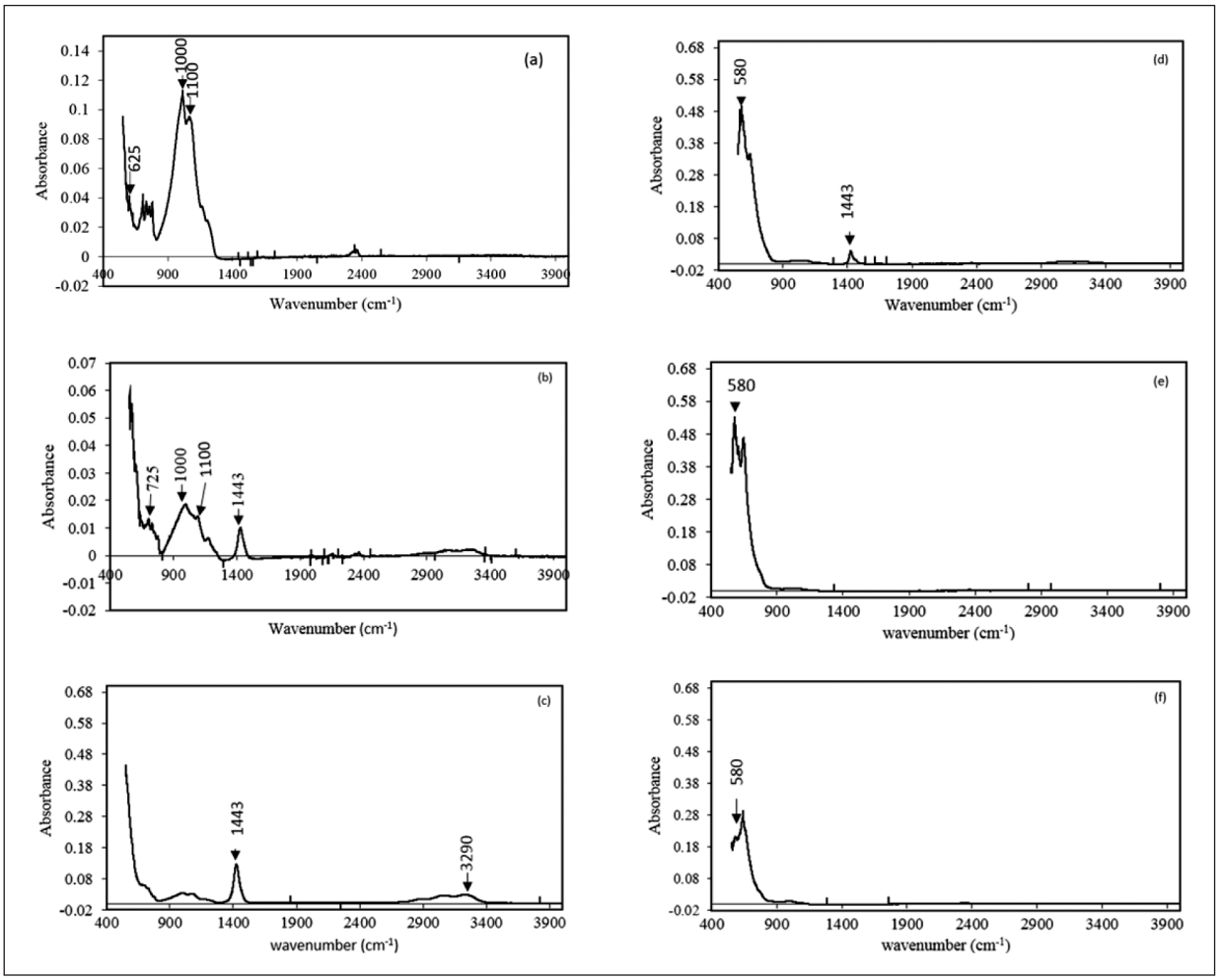

FIGURE 4: FTIR spectra of unreacted petalite and residues after digestion at different temperatures: (a) petalite sample, (b) 200 °C, (c) 300 °C, (d) 400 °C, (e) 500 and (f) 600 °C

The resulting product was washed with water to remove all water-soluble compounds, filtered and dried at 100 °C. These insoluble products were mixed with an excess of sulfuric acid and roasted at 300 °C for 60 min. The resulting product – now a more concentrated slurry – was cooled to room temperature, water was added and the solid dissolved at 80 °C for 20 min.

The increase in temperature between 200 °C to 600 °C increases the reaction efficiency as shown in Figure 5. From Figure 2 it can be seen that ammonium fluorosilicate is decomposed after digestion. From 400 °C up to 600 °C the extraction of lithium was above 95 %. A digestion temperature of 500 °C was recommended as optimal for both economic and efficiency reasons.

The lithium was extracted using an excess acid and high leaching temperatures to ensure complete dissolutions. These conditions were subsequently investigated in more detail. Results are given below.

Acid roasting

Effect of excess acid after digesting petalite with ABF

A number of experiments were done varying the excess sulfuric acid between 0 and 20 % to determine the optimum condition for extraction. According to the results presented in Figure 6, it was established that 5 % excess acid yields 96.5 % extraction, with only a marginal yield increase beyond that.

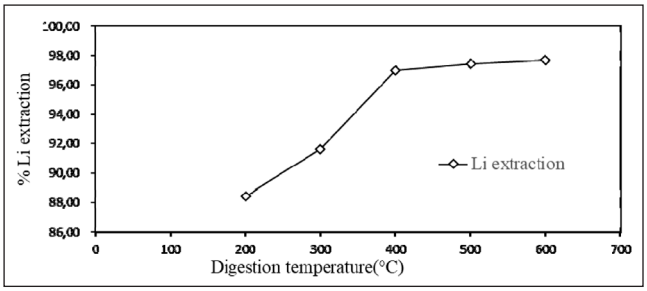

FIGURE 5: Effect of digestion temperature on the lithium extraction with the following conditions: 25 % excess acid, acid roasting temperature 300 °C, water leaching temperature 90 °C, leaching time 60 min, stirring speed 400 rpm and solid-liquid ratio 0.05 g mL^{-1}.

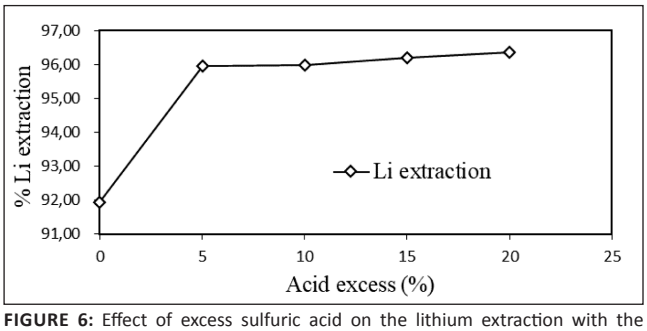

FIGURE 6: Effect of excess sulfuric acid on the lithium extraction with the following conditions: 500 °C digestion temperature, roasting temperature 300 °C, water leaching temperature 90 °C, leaching time 60 min, stirring speed 400 rpm and a solid-liquid ratio of 0.05 g mL^{-1}.

Effect of sulfuric acid roasting temperature

The effect of acid roasting temperature on lithium extraction was determined by investigating the process at 100 °C, 150 °C, and 200 °C. According to the results in Figure 7, an increase in temperature brings about an increase in lithium dissolution. An increase in temperature from 100 °C to 200 °C results in a 1 % increase in lithium dissolution, attributable to the fact that an increase in temperature increases the reaction rate. This difference in yield between 100 °C and 200 °C is minimal. An acid roasting temperature of 100 °C which corresponds to a 96.5 % yield was thus considered sufficient for practical purposes.

Effect of acid roasting time

From Figure 8, roasting time of 30 min was noted to be the optimal for lithium extraction. A lithium extraction approaching 96.5 % was achieved after 30 min at 100 °C roasting temperature.

Leaching

Effect of stirring speed during acid leaching

The effect of agitation on the leaching rate of lithium was investigated in water at 90 °C varying the stirring speed between 100 rpm and 300 rpm. Stirring has a significant influence on the dissolution of lithium, as can be seen from Figure 9, since agitation is essential to keep the solids in suspension and to eliminate the influence of external mass transfer, i.e. of diffusion through the liquid boundary layer. Above 300 rpm, the extraction yield stays practically constant, with a 95.7 % lithium yield.

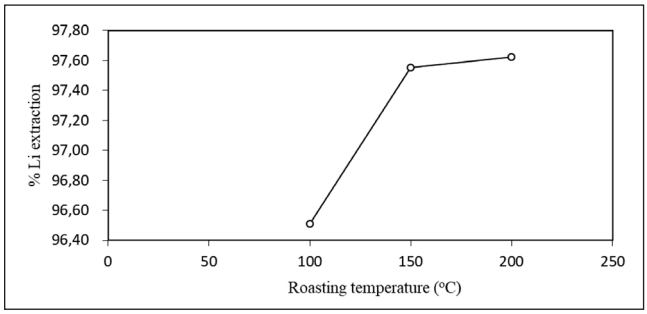

FIGURE 7: Effect of acid roasting temperature on the lithium extraction with the following conditions: excess acid 5 %, roasting time 60 minutes, water leaching temperature 90 °C, leaching time 60 minutes, stirring speed 400 rpm and solid-liquid ratio of 0.05 g mL^{-1}.

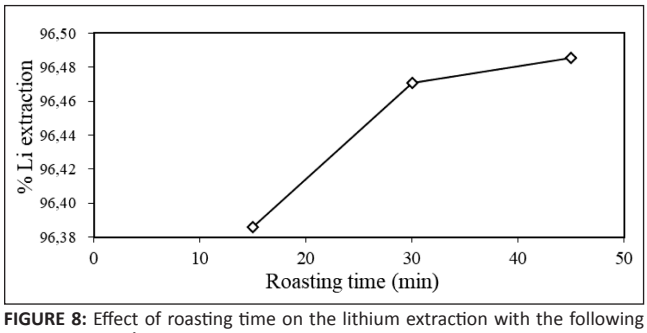

FIGURE 8: Effect of roasting time on the lithium extraction with the following conditions: 500 °C digesting temperature, excess acid 5 %, roasting temperature 100 °C, water leaching temperature 90 °C, leaching time 60 min, stirring speed 400 rpm and a solid-liquid ratio of 0.05 g mL^{-1}.

Effect of solid-liquid ratio during acid leaching

The effect of the solid-liquid ratio (the liquid being water and expressed in g mL^{-1}) was investigated. The results are illustrated in Figure 10. By decreasing the solid-liquid ratio, the viscosity of the system decreased, resulting in easier stirring and an increase in the mass transfer rate at the interface of the solid-liquid surface. For each of the solid-liquid ratios 0.1, 0.067 and 0.05 g mL^{-1} the dissolution yield was almost constant with corresponding extraction yields of 97 %, 96.7 %, and 95.6 %, respectively. Above these values, a drop is observed. A solid-liquid ratio of 0.1 g mL^{-1} was considered optimal.

Effect of water leaching time and temperature

The leaching yield as a function of time was determined at 40 ºC and 80 ºC using a solid-liquid ratio of 0.1 g mL^{-1} and a stirring speed of 300 rpm. From Figure 11, it can be seen that leaching temperature has a significant effect on lithium extraction yield. At 80 ºC the extraction yield is practically constant at just above 96 % between 10 and 40 min. At 40 ºC this is substantially worse, varying between 60 % and 80 % only. Optimal operating parameters are 30 min and at 80 ºC.

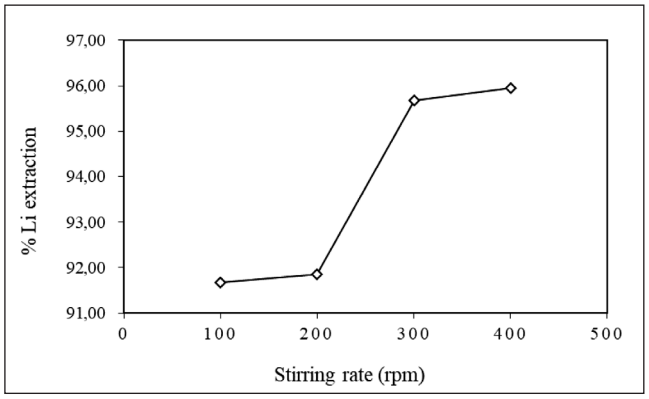

FIGURE 9: Effect of stirring speed on lithium extraction with the following conditions: 500 °C digesting temperature, excess acid 5 %, roasting temperature 100 °C, water leaching temperature 90 °C, leaching time 60 minutes, and a solid-liquid ratio of 0.05 g mL^{-1}.

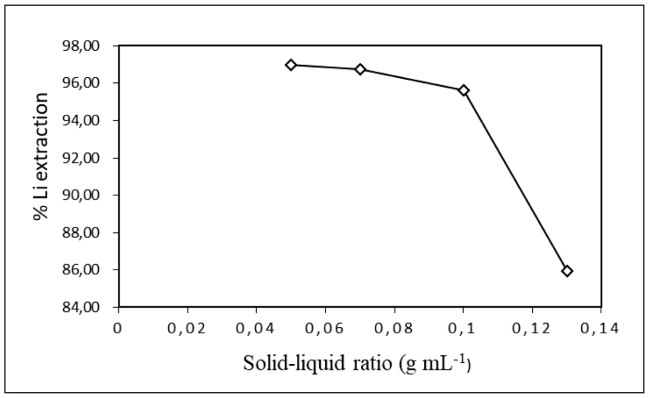

FIGURE 10: Effect of solid-liquid water ratio on the lithium extraction with the following conditions: 500 °C digesting temperature, excess acid 5 %, roasting temperature 100 °C, leaching temperature 90 °C, leaching time 60 min, stirring speed 300 rpm.

Solution purification

Table 3 shows the reduction of impurities in the solution after dissolution and selective precipitation. Calcium carbonate ($CaCO_3$) was effective to precipitate aluminium and iron. The same applies to calcium hydroxide $Ca(OH)_2$ when used to precipitate magnesium. Na_2CO_3 was used to remove excess Ca prior to Li_2CO_3 precipitation. The resulting solution (Li_2CO_3) was evaporated until the concentration of Li was estimated to be more than 5 g L^{-1}, followed by an adjustment of pH value to near 8. The lithium losses in solution during all processes was about 12 %.

Recovery and characterisation of lithium carbonate

The purified leach liquor was subjected to evaporation at 95–100 ºC to precipitate Li_2CO_3. Precipitation was done at this high temperature because the solubility of lithium carbonate decreases with increasing temperature (Wietelmann and Bauer, 2003). Na_2CO_3 is the most effective lithium precipitation chemical; the increased carbonate ion concentration decreases the solubility of Li_2CO_3. A 15 % hot solution of Na_2CO_3 was added to the hot purified leach liquor giving a white precipitate of Li_2CO_3. The precipitate was washed with hot water to remove Na_2SO_4 and other

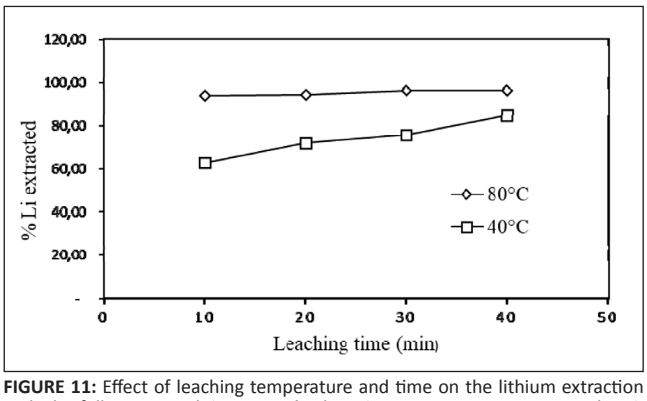

FIGURE 11: Effect of leaching temperature and time on the lithium extraction with the following conditions: 500 °C digesting temperature, excess acid 5 %, roasting temperature 100 °C, solid-liquid ratio 0.1 g mL^{-1}, stirring speed 300 rpm.

TABLE 3: Concentration of elements in solution during the purification process

Solution	pH	Elemental concentration (mg L^{-1})						
		Li	Ca	K	Na	Al	Fe	Mg
Original leach liquor	1.5	4864.6	161.2	252.2	752.6	11887.9	50.1	13.9
Addition of $CaCO_3$ and $Ca(OH)_2$	10.7	3866.5	2241.5	202.1	616.7	566.2	1.9	1.5
Addition of Na_2CO_3	11.2	3453.5	< 0.03	216.1	1601.9	< 0.001	< 0.01	< 0.02
Concentrated leach liquor	8.00	6022.2	50.2	513.4	6580	12.5	< 0.01	2.1
Mother liquor		2486.1						

soluble impurities. Sodium sulfate that also precipitates with other soluble contaminants was washed from the precipitate with hot water during filtration (Lagos and Becerra, 2005). The relevant chemical reaction to precipitate lithium carbonate using Na_2CO_3 is:

$$Li_2SO_{4\,(aq)} + Na_2CO_{3\,(aq)} \rightarrow Li_2CO_{3\,(s)} + Na_2SO_{4\,(aq)} \quad (10)$$

An 86% yield could be obtained.

The product obtained after precipitation was characterised and compared with commercial Li_2CO_3 using X-ray diffractometry. As can be seen, the X-ray diffractograms for the two Li_2CO_3 powders given in Figure 12 are very similar.

The morphology of commercial Li_2CO_3 powder (Figure 13) was compared to the Li_2CO_3 particles synthesised (Figure 14) using SEM. The morphology of both the synthesised and the commercial Li_2CO_3 mostly prismatic with pinacoidal terminations. The particles prepared for this study were smaller and highly agglomerated. The finer size distribution results at higher concentration of lithium in the starting solution. Increasing concentration results in an increase of the nucleation rate by increasing the number of nucleation sites.

Table 4 reports the purity of the synthesised product. It can be seen from the results that the purity of the precipitated product is 98.9 %. Analysis of the precipitate revealed that Na was the major impurity that can be attributed to the excess of Na_2CO_3 used due to insufficient washing.

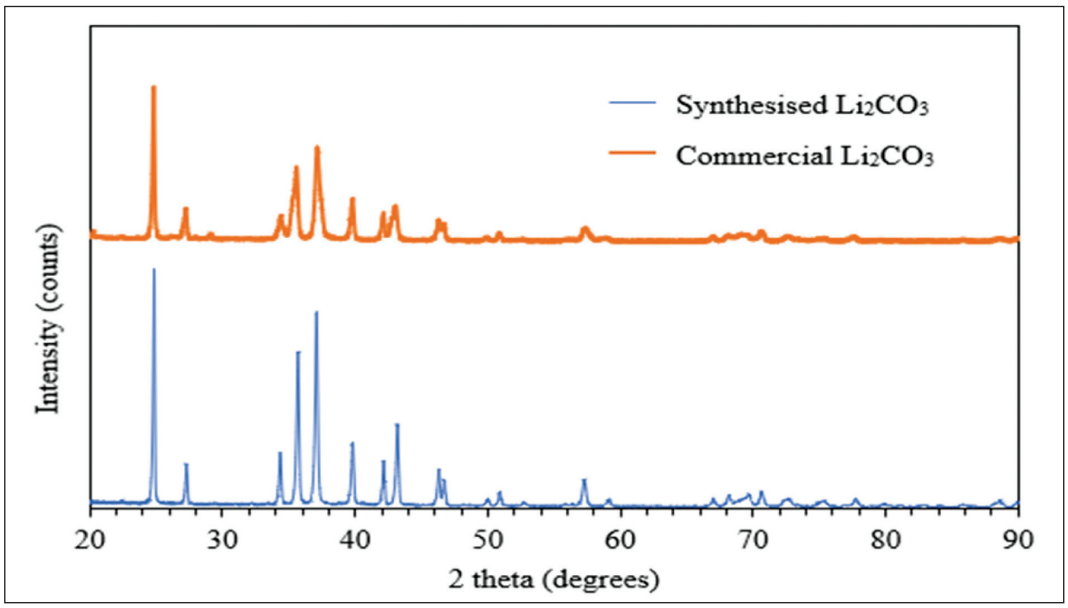

FIGURE 12: X-ray diffractograms of synthesised and commercial Li_2CO_3

FIGURE 13: Secondary-electron SEM image of commercial Li_2CO_3

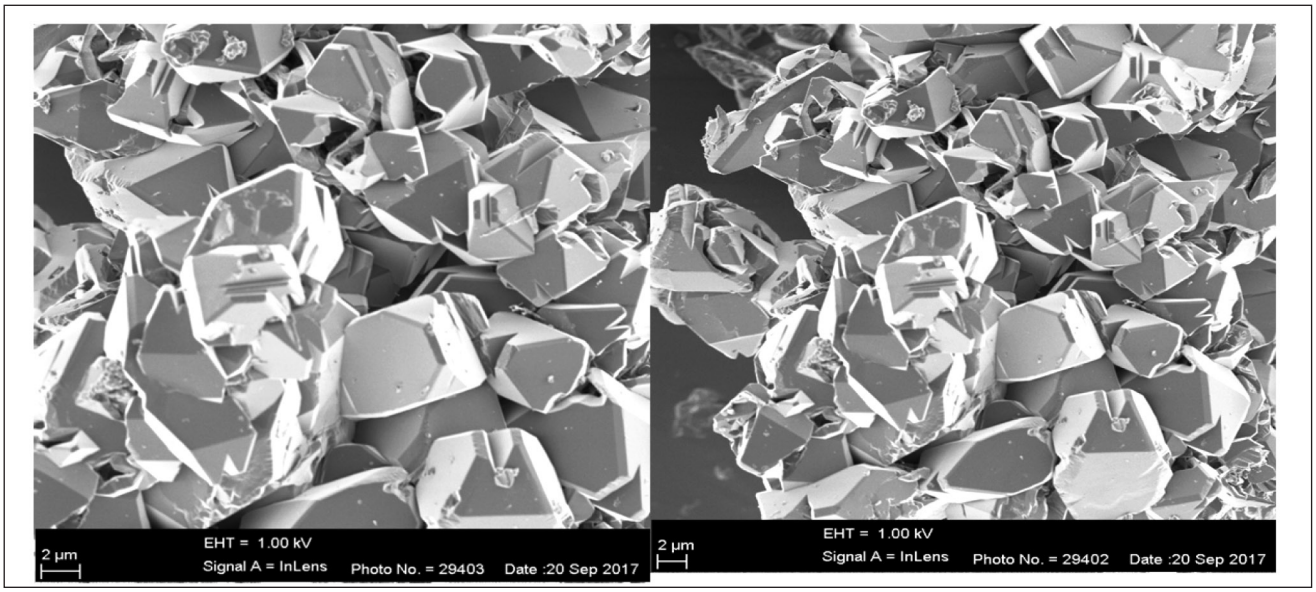

FIGURE 14: Secondary-electron SEM images of in-house synthesised Li_2CO_3

TABLE 4: Composition of synthesised Li_2CO_3

Li_2CO_3 purity (wt %)	Content of major impurities (wt %)					
	Ca	Al	Fe	K	Mg	Na
98.9	0.5	<0.05	<0.01	<0.02	<0.01	0.6

ABF digestion below 100 °C

During the experimental work reported above, it was noted that the ABF-petalite reaction commences even at room temperature. Experiments were subsequently performed to obtain a minimum working temperature. Three-times excess ammonium bifluoride (ABF) was used. The mixture was kept at constant temperatures of 25 °C, 50 °C, 75 °C, and 100 °C, each for 15, 30, 60, 120, 180 and 240 min. The petalite conversion ($\alpha=m/m_o$) was calculated as the ratio of the lithium mass (m) recovered from lithium sulfate solution at time t and the initial mass (m_o) of lithium in the sample. The digesting products were mixed with an excess of acid and roasted. The resulting products were leached and dissolved in water at 80 °C, and ICP-OES was used to determine lithium mass (m). The results are presented in Figure 15 below.

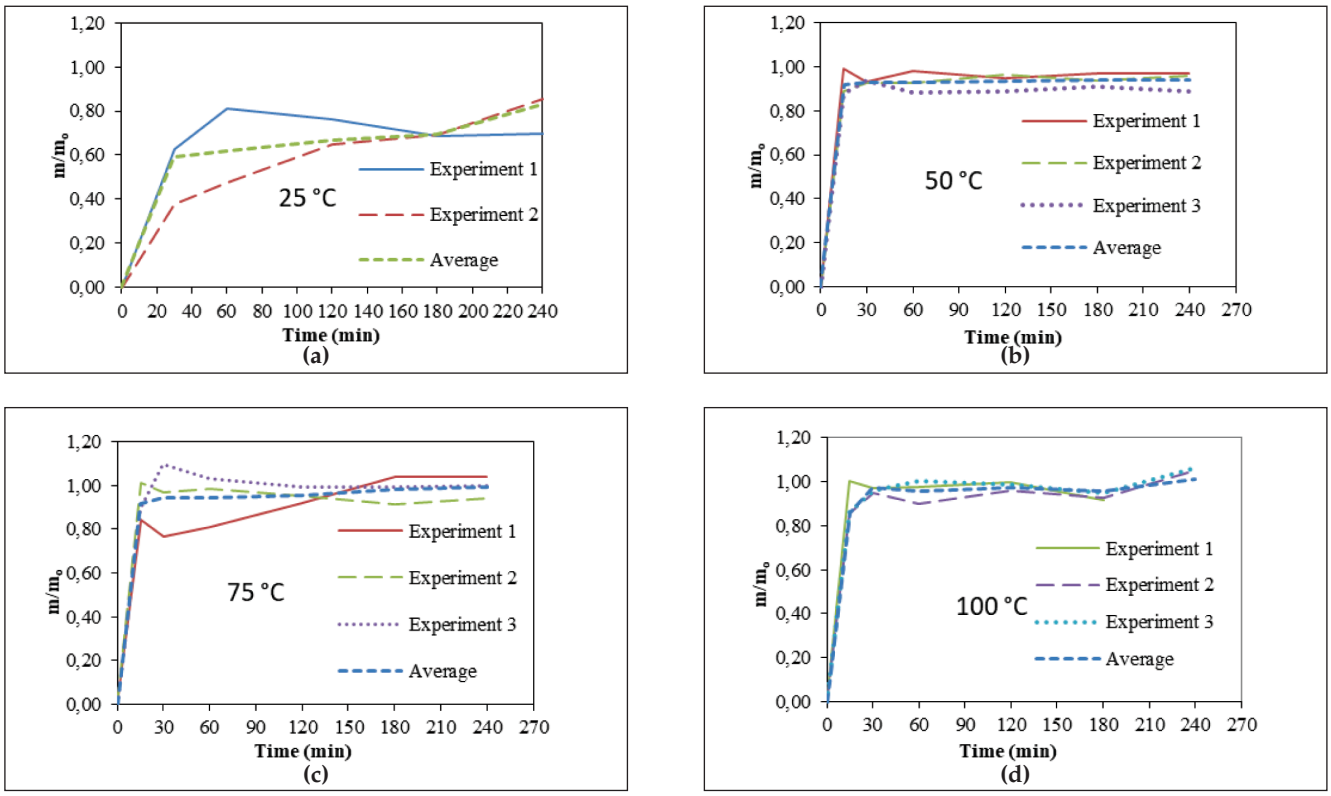

FIGURE 15: Petalite conversion vs time at (a) 25 °C, (b) 50 °C, (c) 75 °C and (d) 100 °C.

It should be noted that in each case the crucible was at room temperature when inserted into the pre-heated furnace (except of course for the 25 °C runs where the crucible was not heated). The reaction times reported include the heating period of the crucible and sample inside the furnace. The times are therefore indicative rather than exact. As seen in Figure 15 (a), the reaction already starts at 25 °C. After 60 min, petalite conversion remains constant at roughly 75 %. Figures 15 (b) to (d) show that the time to equilibrium and the extent of conversion increase at higher temperatures. After 20 min at 50 °C, the petalite conversion remains constant at roughly 91 %. Figure 15 (c) shows that an increase in temperature to 75 °C increases the conversion reaction of petalite to above approximately 95 %. Figure 15 (d) shows that at 100 °C the reaction approaches full conversion.

Figure 16 summarises the main findings from Figure 15, showing the final degree of conversion and total time to reach equilibrium as a function of temperature. The values of α_{Max}, the average degrees of conversion, were calculated using the final three time-data points from the full set of curves for each temperature, as shown in Figure 15. The error bars represent two standard deviations from these average values, i.e., a 2σ, or 68 %, confidence interval. The average time to reach equilibrium was estimated using the first data point in each series at which, within experimental error, the equilibrium composition was reached. The error bars in these cases are 2σ visual estimates. Our overall conclusion is that a temperature of 100 °C for a period of 30 min are safe process-design parameters.

The reactions studied in this research thus commence in the solid state, for all temperatures. As soon as the two solids are mixed, slurry formation and evolution of ammonia are observed, as predicted by Reaction (6). Except at room temperature, the reaction reaches a maximum conversion in less than 40 min. As noted, the maximum yield improves as a function of temperature, with full conversion at 100 °C. We conclude that the reaction is not diffusion limited, as might be expected. It appears to reach a thermodynamic limit, dictated by the equilibrium position in the semi-aqueous environment of the slurry. Figure 17 (a) and (b) show the X-ray diffractograms of the petalite concentrate before and after reaction with ABF at 100 °C. After reaction, the solid contains the solid fluorides as discussed.

Recovery of lithium compounds is readily achieved via the sulfuric acid roasting, leaching, and precipitation, as for the high-temperature material, as described in the sections above.

Conclusion

Ammonium bifluoride is a facile digestion agent for petalite, bypassing the usual high-temperature conversion of the mineral to β-spodumene. The process works at surprisingly low temperatures, with the reaction observed even at room temperature with slurry formation due to the release of water. Below the melting point of ABF, the main products are LiF, AlF_3, K_2NaAlF_6, and $(NH_4)_2SiF_6$. $(NH_4)_2SiF_6$ decomposes readily to form ammonia and gaseous SiF_4. At higher temperatures, the products are cryolithionite ($Li_3Na_3Al_2F_{12}$) and eucryptite ($LiAlSiO_4$). The fluoride solids are not readily soluble in water and may be roasted in sulfuric acid, then leached, with 99 % pure lithium carbonate easily recovered from the aqueous phase.

Economic viability has not been considered in much detail

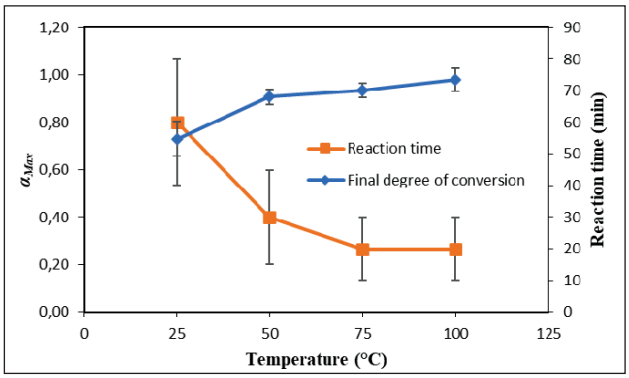

FIGURE 16: Final degree of conversion (α_{max}) of Zimbabwean petalite at different temperatures and corresponding time to reach α_{max}.

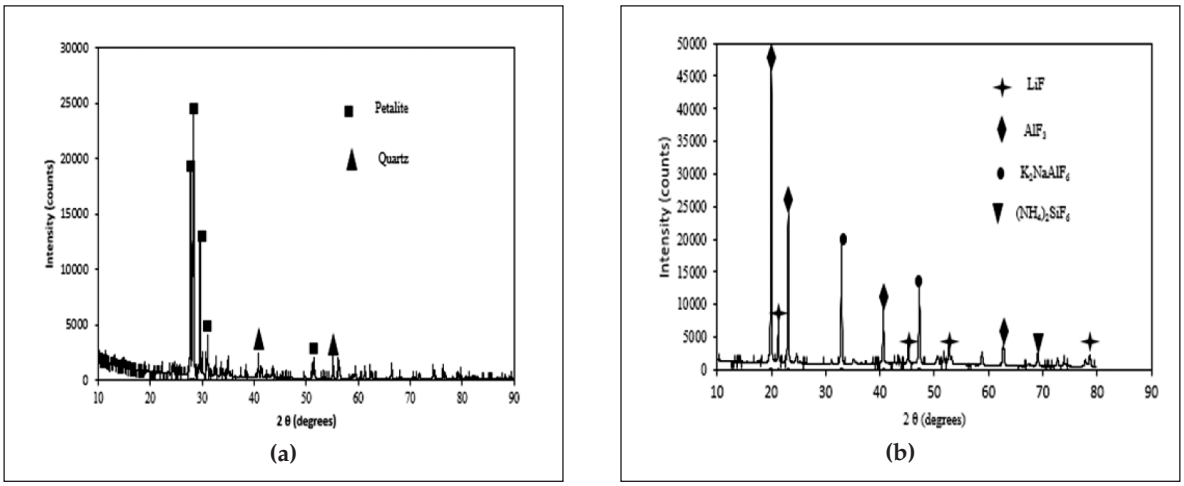

FIGURE 17: X-ray diffractogram of Zimbabwean petalite (a) before and (b) after reaction with NH_4HF_2.

at this stage. Most likely, consideration will have to be given to the unwanted silicon and aluminium fluorides for a profitable process. The ammonium hexafluorosilicate decomposes readily into ammonia, AHF, and SiF_4. The ammonia and AHF may be recovered, in principle, and recycled as ABF. Silicon tetrafluoride, generally found as effluent in the phosphate industry in the form of fluosilicic acid, may be reduced using an appropriate metal to yield usable solid silicon. The metal fluoride produced may in its turn be employed along with e.g. its oxide for the production of the element. Successful use of the byproducts may result in the research reported in this paper being more than a laboratory curiosity.

Acknowledgements

We would like to thank Bikita Minerals (Pvt) Ltd for providing the petalite samples which were used in this research work, the Fluorochemical Expansion Initiative (FEI) for financial assistance, and Dr Kokkie Swanepoel for ideas around the recycling of the waste streams.

References

Andreev, V.A., Buynovskiy, A.S., Andreev, A.A., Dyachenko, A.N. 2007a. Topaz concentrate desiliconization with ammonium bifluoride. Bulletin of the Tomsk Polytechnic University, 311, 27-31.

Andreev, V.A., Buynovskiy, A.S., Dyachenko, A.N., Kraidenko, R.I. 2007b. Studying the utilization techniques of ammonium heksafluorosilicate. Bulletin of the Tomsk Polytechnic University, 311, 31-34.

Aylmore, M.G., Merigot, K., Rickard, W.D. 2018. Assessment of a spodumene ore by advanced analytical and mass spectrometry techniques to determine its amenability to processing for the extraction of litium. Minerals Engeneering, 119, 137-148. https://doi.org/10.1016/j.mineng.2018.01.010.

Du Plessis, W., Pienaar, A.D., Postma, C.J., Crouse, P.L. 2016. Effect of the value of x in NH4F· xHF on the digestion of plasma-dissociated zircon. International Journal of Minereral Processing, 147, 43-47. https://doi.org/10.1016/j.minpro.2016.01.002.

Duke, C.V., Miller, J.M., Clark, J.H., Kybett, A.P. 1990. 19F mas NMR and FTIR analysis of the adsorption of alkali metal fluorides onto alumina. Journal of molecular catalysis, 62, 233-242. https://doi.org/10.1016/0304-5102(90)85216-5.

Garrett, D.E., 2004. Handbook of litium and natural calcium chloride, UK, vol.I.Elsevier Book,Elsevier Ltd. https://doi.org/10.1016/B978-012276152-2/50038-4.

Guo, H., Kuang, G., Wan, H., Yang, Y., YU, H.-Z., Wang, H.D. 2019. Enhanced acid treatment to extract litium from lepidolite with a fluorine-based chemical method. Hydrometallurgy, 183, 9-19. https://doi.org/10.1016/j.hydromet.2018.10.020.

Hien-Dinh, T.T., Luong, V.T., Gieré, R., Tran, T. 2015. Extraction of litium from lepidolite via iron sulphide roasting and water leaching. Hydrometallurgy, 153, 154-159. https://doi.org/10.1016/j.hydromet.2015.03.002.

Hoshino, D., Adachi, S., 2007. Stain Etching Characteristics of Silicon (001) Surfaces in Aqueous HF/ K2Cr2O7 Solutions. Journal of The Electrochemical Society, 154, E139-E144. https://doi.org/10.1149/1.2767852.

House, J.E., Engel, D.A. 1983. Decomposition of ammonium bifluoride and the proton affinity of the bifluoride ion. Thermochimica Acta, 66, 343-345. https://doi.org/10.1016/0040-6031(93)85045-B.

Hui, G., Yu, H.Z., Zhou, A.A. 2019. Kinetics of leaching litium from α-spodumene in enhanced acid treatment using HF/H2SO4 as medium. Transactions of Nonferrous Metals Society of China, 29, 407-415. https://doi.org/10.1016/S1003-6326(19)64950-2.

Jandová, J., Dvořák, P., Vu, H.N. 2010. Processing of zinnwaldite waste to obtain Li2CO3. Hydrometallurgy, 103, 12-18.https://doi.org/10.1016/j.hydromet.2010.02.010.

Kabacelik, I., Ulug, B. 2008. Further investigation on the formation mechanisms of (NH4) 2SiF6 synthesized by dry etching technique. Applied Surface Science, 254, 1870-1873. https://doi.org/10.1016/j.apsusc.2007.08.064.

Kondás, J., Jandová, J., Nemeckova, M. 2006. Processing of spent Li/MnO2 batteries to obtain Li2CO3. Hydrometallurgy, 84, 247-249. https://doi.org/10.1016/j.hydromet.2006.05.009.

Kuang, G., Chen, Z.B., Guo, H., Li, M.H. 2012. Litium Extraction Mechanism from α-Spodumene by Fluorine Chemical Method. Advanced Materials Research, 524-527, 2011-2016. https://doi.org/10.4028/www.scientific.net/AMR.524-527.2011.

Kuang, G., Liu, Y., Li, H. 2018. hydrometExtraction of litium fromβ-spodumene using sodium sulfate solution. Hydrometallurgy, 177, 49-56. https://doi.org/10.1016/j.hydromet.2018.02.015.

Lagos, S., Becerra, R. 2005. Methodology for the recovery of litium from litium titanate. Journal of Nuclear Materials, 347, 134-139. https://doi.org/10.1016/j.jnucmat.2005.08.013.

Linnen, R.L., Van Lichtervelde, M., Černý, P. 2012. Granitic pegmatites as sources of strategic metals. Elements, 8, 275-280. https://doi.org/10.2113/gselements.8.4.275.

Nel, J.T., Du Plessis, W., Nhlabathi, T.N. 2011. Reaction kinetics of the microwave enhanced digestion of zircon with ammonium acid fluoride. Journal of Fluorine Chemistry, 132, 258-262. https://doi.org/10.1016/j.jfluchem.2011.01.012.

Nhlabathi, T.N., Nel, J.T., Puts, G.J., Crouse, P.L. 2012. Microwave digestion of zircon with ammonium acid fluoride: Derivation of kinetic parameters from non-isothermal reaction data. International Journal of Mineral Processing, 114-117, 35-39. https://doi.org/10.1016/j.minpro.2012.09.002.

Retief, W.L., Nel, J.T., Du Plessis, W., Crouse, P.L. 2014. Treatment of zirconia-based material with ammonium bi-fluoride. Google Patents 0011329 A1, assigned to South African Nuclear Energy Corporation Limited.

Rosales, G.D., Del Carmen Ruiz, M., Rodriguez, M.H. 2013. Alkaline metal fluoride synthesis as a subproduct of β-spodumene leaching. Hydrometallurgy, 139, 73-78. https://doi.org/10.1016/j.hydromet.2013.07.008.

Rosales, G.D., Del Carmen Ruiz, M., Rodriguez, M.H. 2016. Study of the Extraction Kinetics of Litium by leaching -Spodumene with Hydrofluoric Acid. Minerals, 6,98, 1-12. https://doi.org/10.3390/min6040098.

Sitando, O., Crouse, P.L. 2012. Processing of a Zimbabwean petalite to obtain litium carbonate. International Journal of Mineral Processing, 102, 45-50. https://doi.org/10.1016/j.minpro.2011.09.014.

Wietelmann, U., Bauer, R. 2003. Litium and Litium Compounds. Ullmann's Encyclopedia of Industrial Chemistry, vol. 20. Wiley-VCH Verlag GmbH & Co. Weinheim, Germany.